Relaxation and polarization effects in photodetachment of the negative iodide ion

M. Kutzner, J. T. Brown, and J. Thorarinson*
Department of Physics, Andrews University, Berrien Springs, Michigan 49104, USA
(Received 17 July 2003; published 23 October 2003)

Photodetachment cross sections have been calculated for the $5p$, $4d$, and $4p$ subshells of the negative iodide ion, I^-, in the relativistic random-phase approximation (RRPA) and modifications of the RRPA that allow for the inclusion of relaxation and core-polarization effects. Total and partial photodetachment cross sections are compared with experimental measurements to gauge the effectiveness of the various approximations. Branching ratios and photoelectron angular-distribution asymmetry parameters are also presented. Core-polarization effects are found to partially cancel relaxation effects.

DOI: 10.1103/PhysRevA.68.042713 PACS number(s): 32.80.Gc

I. INTRODUCTION

Studies of photodetachment of negative-ion systems highlight the significance of various electron correlation effects. Examination of such systems provides insight into many-body effects in the absence of a long-range Coulomb attraction by the nucleus seen in neutral atoms or positive ions. The negative iodide ion is a good species for demonstrating many-body effects as reported in the review by Ivanov [1]. Near-threshold measurements of photodetachment cross sections of the negative iodide ion were reported by Mandl and Hyman [2] as well as by Neiger [3]. Absorption spectra of I_2 (gaseous and solid) [4] and CH_3I [5] have also been measured. Lindle *et al.* [6] partitioned the total photoabsorption cross section of CH_3I into partial $4d$ and "$4p$" cross sections and measured angular-distribution asymmetry parameters. Several theoretical methods have been successfully used in studying many-body effects in neutral atoms, and have also been applied to valence photodetachment of negative ions. Such techniques include the many-body perturbation theory (MBPT) [7], close-coupling [8], *R*-matrix [9], multichannel quantum-defect theory [10], and the relativistic random-phase approximation (RRPA) [11]. Radojević and Kelly [12] extended RRPA calculations of outer-shell photodetachment of I^- to include relaxation effects in photodetachment of inner-shell $4d$ electrons. They reported the presence of a "giant resonance" above the $4d$ threshold similar to that of the neighboring elements Xe and Ba. Relaxation and polarization effects in the $4d$ subshell of barium and xenon were shown to bring calculations [13] in better agreement with $4d$ photoemission measurements.

The present study investigates the effects of core relaxation and polarization in the photodetachment process of I^- using the modification of RRPA (RRPARP). Kutzner *et al.* reported the effects of relaxation and polarization on the valence and inner shells of F^- and Br^- [14] and Cl^- [15]. It was found that the inclusion of a polarization potential partially canceled the effects of relaxation. The methods used are described in Sec. II and the results are reported in Sec. III. Some of the implications of the paper are discussed in Sec. IV.

II. METHODS

The RRPA has proven to be a successful method for including the effects of interchannel coupling in calculations of photoionization parameters of closed-shell systems [16]. Radojević, Kutzner, and Kelly [17] modified the RRPA to include relaxation effects (RRPAR) by calculating the continuum orbitals in the potential of the relaxed core. For a neutral atom, the relaxed core is a positive ion whereas for photodetachment of negative ions the relaxed core is the neutral atom. In RRPARP we add a polarization potential of the form [18]

$$V_{pol}(r) = -\frac{\alpha_d}{2(r^2+h^2)^2}, \tag{1}$$

where α_d is the static dipole polarizability of the core and h is a cutoff radius (approximately the size of the valence electron cloud) which prevents the potential from becoming unmanageable for small radii.

Similar polarization potentials have been used previously for neutral atoms in the eigenchannel *R*-matrix [19] with the polarizability and cutoff radius treated as parameters determined semiempirically by optimizing the fitting agreement between the calculated and experimental energy levels. Such an approach is not possible when dealing with negative halide ions not possessing bound-excited states.

The large polarizability for the neutral iodine atom is 33.00 a.u. [20]. The cutoff radius h was determined by requiring that $V_{pol}(0)$ be approximately equivalent to the energy correction of the subshell $n\ell$ orbitals [18]. This condition may be expressed as

$$V_{pol}(0) \approx \Delta E_{\mathrm{SCF}}(n\ell) - |\varepsilon_{n\ell}|, \tag{2}$$

where $\varepsilon_{n\ell}$ is the Dirac-Hartree-Fock (DHF) eigenvalue and ΔE_{SCF} is the absolute value of the difference between the total ground-state self-consistent-field energies of the iodide ion and the neutral iodine atom. Equations (1) and (2) may be combined to determine the value for the parameter $h_{n\ell}$, yielding

*Present address: Department of Physics and Astronomy, Dartmouth College, Hanover, New Hampshire 03755-3528, USA.

TABLE I. Photoionization thresholds (in a.u.) for the various subshells of the negative iodide ion. The second column lists the absolute values of single-particle eigenvalues from a Dirac-Hartree-Fock (DHF) calculation using the code of Ref. [21]. The third column lists the absolute values of the difference between self-consistent-field calculations of total energy of the neutral atom and the ion (ΔE_{SCF}). The fourth column lists the cutoff radius, h, for the subshells studied.

Subshell J	DHF eigenvalues	ΔE_{SCF}	Cutoff radius, h
$5p_{3/2}$	0.154 588 8	0.080 078 1	4.71
$5p_{1/2}$	0.113 525 3	0.115 234 4	
$5s_{1/2}$	0.608 437 4	0.558 593 8	
$4d_{5/2}$	1.980 696 2	1.762 207 0	2.95
$4d_{3/2}$	2.048 162 5	1.826 660 2	
$4p_{3/2}$	5.156 576 2	4.910 644 5	2.86
$4p_{1/2}$	5.575 483 3	5.320 312 5	
$4s_{1/2}$	7.465 663 4	7.200 683 6	

$$h_{n\ell}=\sqrt[4]{-\alpha_d/\{2[\Delta E_{\mathrm{SCF}}(n\ell)-|\varepsilon_{n\ell}|]\}}. \tag{3}$$

Table I lists the values of the energies used in these calculations. The energy correction of Eq. (2) was determined using the Oxford multiconfiguration Dirac-Fock computer code of Grant *et al.* [21].

Photodetachment transition matrix elements were calculated using the RRPA code of Johnson *et al.* [16], the RRPAR, which is a modified RRPA including relaxation effects [17], and the RRPARP, which includes relaxation effects as well as the polarization potential of Eq. (1) added to the single-particle potential for the calculation of RRPA excited-state orbitals. All I^- calculations included interchannel coupling between 20 channels in *jj* coupling, namely,

$$5p_{3/2}\rightarrow \epsilon d_{5/2},\ \epsilon d_{3/2},\ \epsilon s_{1/2},$$

$$5p_{1/2}\rightarrow \epsilon d_{3/2},\ \epsilon s_{1/2},$$

$$5s_{1/2}\rightarrow \epsilon p_{3/2},\ \epsilon p_{1/2},$$

$$4d_{5/2}\rightarrow \epsilon f_{7/2},\ \epsilon f_{5/2},\ \epsilon p_{3/2},$$

$$4d_{3/2}\rightarrow \epsilon f_{5/2},\ \epsilon p_{3/2},\ \epsilon p_{1/2},$$

$$4p_{3/2}\rightarrow \epsilon d_{5/2},\ \epsilon d_{3/2},\ \epsilon s_{1/2},$$

$$4p_{1/2}\rightarrow \epsilon d_{3/2},\ \epsilon s_{1/2},$$

$$4s_{1/2}\rightarrow \epsilon p_{3/2},\ \epsilon p_{1/2}.$$

Traditionally, the Dirac-Hartree-Fock eigenvalue energies are used as thresholds for the RRPA [16]. To facilitate comparisons with the experiments, we used experimental thresholds listed in Table I. Although this undermines the gauge invariance of the strict RRPA results, the length and velocity discrepancy is largely removed when relaxation effects are included in the RRPAR and RRPARP. The cross-section results are presented as the geometric mean of length and velocity since the geometric mean is less sensitive to the effects of ground-state correlation as demonstrated by Hansen [22].

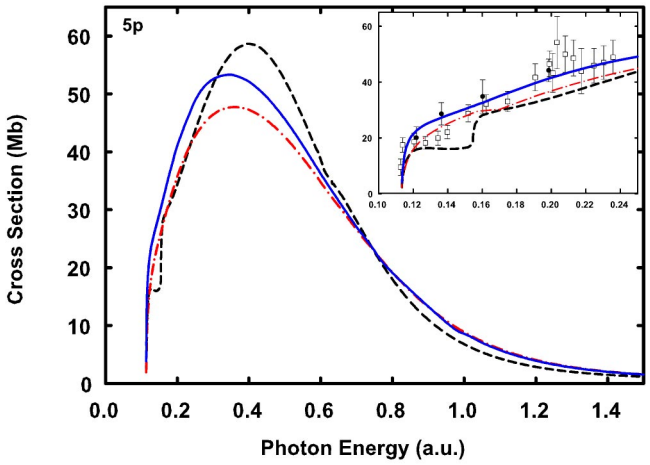

FIG. 1. Photodetachment cross section for the $5p$ subshell of I^-. The dashed line is RRPA; the dot-dashed line is the RRPAR; the solid line is RRPARP, which includes relaxation and polarization effects. In the inset is shown the photodetachment cross section for photon energies close to threshold. Open squares and closed circular data points are experimental measurements from Refs. [2] and [3], respectively.

III. RESULTS

A. The $5p$ subshell

The valence photodetachment cross sections for I^- are shown in Fig. 1. The RRPA and RRPAR of the total cross section calculation are nearly identical to results reported by Radojević and Kelly [12] except that our calculations include interaction with $4p$ and $4s$ channels. The effects of core relaxation effectively displace oscillator strength from near threshold to higher energies, leading to a lower slope for the cross section near the thresholds. But previous work has shown [14,15] that including only relaxation effects in valence photodetachment, without the partial cancellation contributed by polarization effects, produces unbalanced results. The inclusion of polarization effects (RRPARP) increases the value of the cross section from the threshold region to the cross-section peak. It was previously reported that in the case of F^- and Cl^- [14] and Br^- [15], including the polarization potential effects increases the photodetachment cross section and partially cancels the effects of core relaxation.

In the RRPA, distinct spin-orbit splitting is seen between the $5p_{3/2}$ and $5p_{1/2}$ thresholds due to the sizable value of Z. A trend of increasing spin-orbit splitting in threshold energies with increased Z may be noted among the halides [14,15] with an extreme splitting reported for At^- [23]. Including relaxation effects tends to remove this stepwise feature.

The branching ratios, $\gamma=\sigma(5p_{3/2})/\sigma(5p_{1/2})$, are shown in Fig. 2. Spin-orbit splitting causes the branching ratio to be larger than the statistical value of 2 near threshold. For energies close to the threshold, the branching ratio is much larger than the statistical ratio because the partial cross sec-

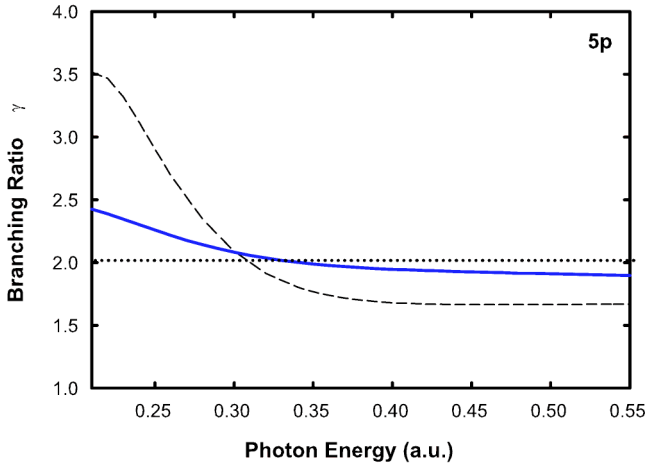

FIG. 2. Branching ratio, $\gamma = \sigma(5p_{3/2})/\sigma(5p_{1/2})$, for I^-. Dashed line is RRPA and the solid line is representative of both RRPAR and RRPARP. The statistical value of 2 is indicated by the dotted line.

tions are increasing with photoelectron energy. For higher energies where the cross sections are decreasing, the branching ratio becomes less than the statistical ratio where it remains out to very high energies, eventually approaching the value of 2.0.

B. The 4*d* subshell

The inner-shell $4d$ photoionization spectra of atomic lanthanides and the preceding elements (i.e., Xe and Ba) are characterized by a shape resonance often referred to as a ''giant resonance.'' This shape resonance results from the interaction of the outgoing photoelectron with a centripetal barrier. At higher energies, the $4d \rightarrow \varepsilon f$ dipole matrix element experiences a change in sign and falls to a Cooper minimum. The total cross sections for the $4d$ subshell are shown in Fig. 3. Similarly to the $4d$ subshell of xenon [12], the cross section rises rapidly from the threshold to a gentle

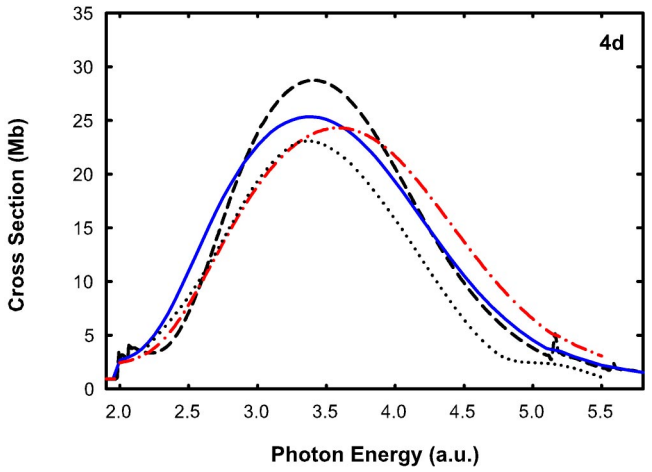

FIG. 3. The total cross section for the $4d$ subshell of I^-. The dashed line is RRPA; the dot-dashed line is RRPAR; the solid line is RRPARP; the dotted line is the ultraviolet absorption spectrum of I_2 from Ref. [4].

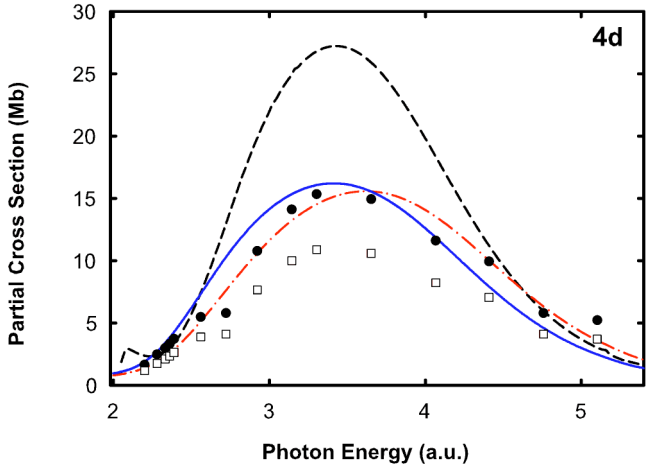

FIG. 4. The partial cross section for the $4d$ subshell of I^-. The dashed line is RRPA; the dot-dashed line is RRPAR; the solid line is RRPARP; the solid dots and open squares represent experimental CH_3I data from Lindle *et al.* [6] scaled to absolute cross sections from Refs. [4] and [5], respectively.

peak, and then rapidly decreases to a Copper minimum. Including relaxation effects (RRPAR) reduces the cross section below the peak, and shifts the peak of relaxation to a slightly higher energy. Similar results were reported for Xe [12] and Ba [13]. It is noteworthy that the electrons in the negative iodide ion are less tightly bound than for a neutral atom like xenon, and the removal of an electron should cause larger rearrangement effects as stated by Radojević and Kelly [12]. Including polarization effects provides a more accurate representation of the cross section. Polarization of the total cross section (RRPARP) partially cancels the relaxation effects (RRPAR), shifting the peak back to a lower energy and increasing the cross section near threshold. The measurements

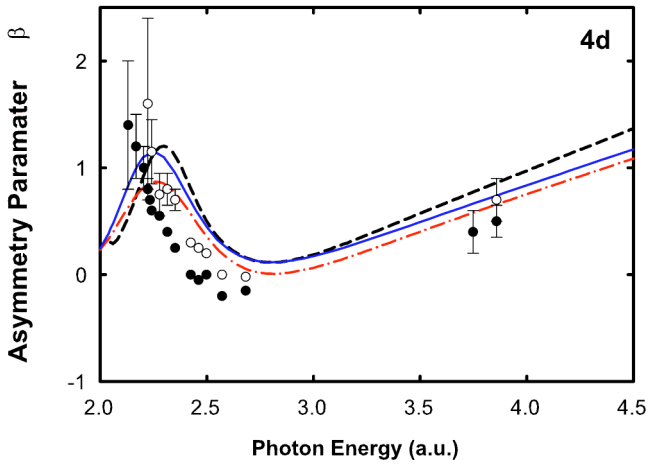

FIG. 5. Angular-distribution asymmetry parameter, β_{4d}, for I^-. The $4d_{3/2}$ and $4d_{5/2}$ theoretical results are presented as an average weighted by the partial cross sections. The dashed line is RRPA; the dot-dashed line is RRPAR; the solid line is RRPARP; the experimental data are from Ref. [6] with open circles representing the $4d_{3/2}$ component and closed circles representing the $4d_{5/2}$ component.

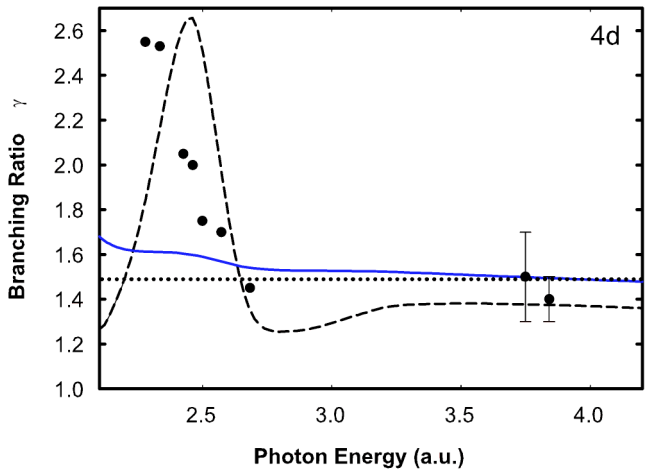

FIG. 6. Branching ratio, $\gamma = \sigma(4d_{5/2})/\sigma(4d_{3/2})$, for I^-. Dashed line is RRPA and the solid line is representative of both RRPAR and RRPARP. The statistical value of 1.5 is indicated by the dotted line.

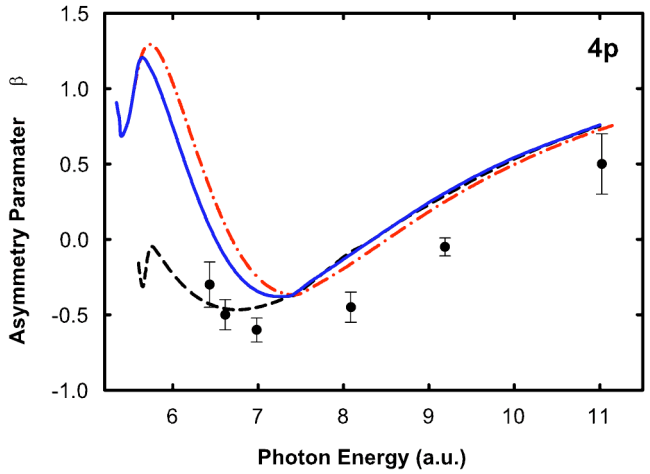

FIG. 8. Angular-distribution asymmetry parameter, β_{4p}, for I^-. The dashed line is RRPA; the dot-dashed line is RRPAR; the solid line is RRPARP; the experimental data are of $4p$ from CH_3I, Ref. [5].

of Comes *et al.* [4] of I_2 gas are shown for comparison, although there is considerable uncertainty in the overall scale. The experiment also demonstrates that solidification has little influence on the continuous absorption in the $4d \rightarrow \varepsilon f$ continuum with the implication that I^- should have a very similar absorption cross section. Figure 4 is a comparison of $4d$ partial cross sections. The inclusion of overlap integrals in the RRPAR and RRPARP reduce the partial cross section by approximately 17%, independent of energy similar to that noted for barium [13]. The measured partial cross section is also shown of CH_3I as reported by Lindle *et al.* [6] as scaled to the total cross sections of O'Sullivan [5] and the I_2 cross section of Comes [4].

The angular-distribution asymmetry parameter, β_{4d}, is shown in Fig. 5. When a subshell is split by spin-orbit splitting into two different levels $j = \ell \pm 1/2$, it is conventional to calculate the average of the two asymmetry parameters weighted according to the partial cross sections. The experimental parameters [6] are presented separately for each j level. As in the case of the total cross section of the initial state ion and the relaxed final state, the inclusion of relaxation and polarization effects causes substantial changes in the dipole matrix elements. Apart from the choice of $4d$ threshold, the RRPARP closely agrees with RRPA.

The branching ratios for $\gamma = \sigma(4d_{5/2})/\sigma(4d_{3/2})$ are shown in Fig. 6. Spin-orbit splitting causes the branching ratio to be larger than the statistical value of 1.5 near threshold. At high energy the RRPA result falls well below the statistical value, while the RRPAR and RRPARP results approach the statistical value from above. The RRPAR and RRPARP are nearly indistinguishable and are plotted as one curve. Interestingly, the sharper peak in the RRPA cross sections results in a larger deviation in γ from the statistical value in better agreement with the measured CH_3I result [6] than the models which include relaxation.

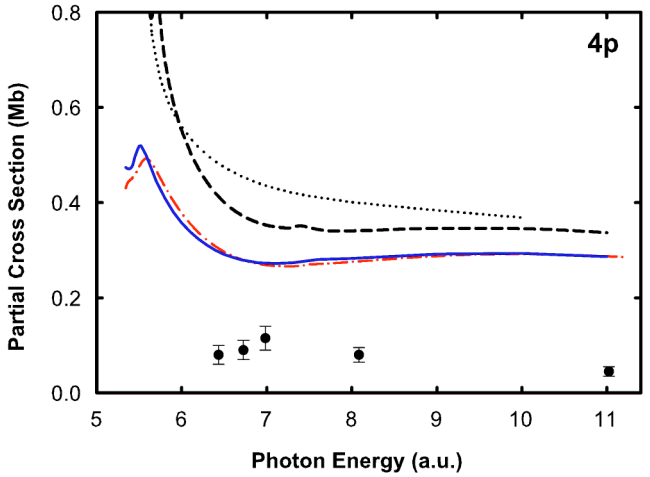

FIG. 7. The partial cross section for the $4p$ subshell of I^-. The dashed line is RRPA; the dot-dashed line is RRPAR; the solid line is RRPARP; the dotted line is Dirac-Hartree-Fock calculation and the experimental measurements of $4p$ in CH_3I of Ref. [5].

C. The $4p$ subshell

The partial cross sections for the $4p$ subshell are presented in Fig. 7 in the Dirac-Hartree-Fock, RRPA, RRPAR, and RRPARP calculations. The effect of interchannel coupling, noted by comparing the Dirac-Hartree-Fock result with that of the RRPA, is to enhance the cross section near threshold. Relaxation effects reduce the partial cross section at all energies. Polarization has little affect on the partial cross section. Lindle *et al.* [6] interpret the "$4p$" result as primarily due to the $4d4f$ final state and not truly representative of the direct removal of electrons from the $4p$ subshell which could explain why the theoretical results are all much larger in magnitude than experiment. The angular-distribution asymmetry parameters, β_{4p}, are shown in Fig. 8.

IV. CONCLUSIONS

Relaxation and polarization effects have been found to play a large role in the photodetachment of I^- from the va-

lence subshell down to the $4d$ subshell, with little effect noted for the $4p$ subshell. The loosely bound outer electrons are easily rearranged by the presence of a $4d$ hole and are readily distorted by an outgoing photoelectron. In general, polarization effects are found to partially cancel relaxation effects, indicating that the photoelectron partially fills the hole. Substantial effects had been anticipated for the $4d$ subshell since both xenon and barium have been showcases for relaxation and polarization studies in the past. Comparisons with experimental total and partial cross sections for I_2 [4] and CH_3I [5,6] appear to be in reasonable agreement with the RRPARP for inner shells, perhaps because of the relative isolation from outer electrons involved in bonding.

The calculations of the photodetachment cross section do not agree with the scaling of the experimental measurements of $4p$ photoionization of CH_3I [6]. The closer agreement between the RRPA-type and the measured $4p$ angular-distribution asymmetry parameter [6] may be understood by considering that the asymmetry parameter depends on ratios of matrix elements, according to the Cooper-Zare [24] treatment, rather than on absolute scale.

ACKNOWLEDGMENTS

We wish to thank Walter Johnson for the use of the RRPA computer code. This work was supported by Grant No. PHY-0099526 of the National Science Foundation and by the Office of Scholarly Research of Andrews University.

[1] V. K. Ivanov, J. Phys. B **32**, R80 (1999).
[2] A. Mandl and H. A. Hyman, Phys. Rev. Lett. **31**, 417 (1973).
[3] M. Neiger, Naturforsch A: Phys. Sci. **30**, 474 (1975).
[4] F. J. Comes, U. Nielsen, and W. H. E. Schwarz, J. Chem. Phys. **58**, 2230 (1973).
[5] G. O'Sullivan, J. Phys. B **15**, L327 (1982).
[6] D. W. Lindle *et al.*, Phys. Rev. A **30**, 239 (1984).
[7] T. Ishihara and T. C. Foster, Phys. Rev. A **9**, 2350 (1974); Z. D. Qian and H. P. Kelly (private communication).
[8] D. L. Moores and D. W. Norcross, Phys. Rev. A **10**, 1646 (1974); K. T. Taylor and D. W. Norcross, *ibid.* **34**, 3878 (1986).
[9] Ramsbottom, K. L. Bell, and K. A. Berrington, J. Phys. B **26**, 4399 (1993); **27**, 2905 (1994); C. A. Ramsbottom and K. L. Bell, *ibid.* **28**, 4501 (1995).
[10] C. H. Greene, Phys. Rev. A **42**, 1405 (1990); H. R. Sadeghpour, C. H. Greene, and M. Cavagnero, *ibid.* **45**, 1587 (1992); C. Pan, A. F. Starace, and C. H. Greene, J. Phys. B **27**, L137 (1994).
[11] V. Radojević, H. P. Kelly, and W. R. Johnson, Phys. Rev. A **35**, 2117 (1987).
[12] V. Radojević and H. P. Kelly, Phys. Rev. A **46**, 662 (1992).
[13] M. Kutzner, Z. Altun, and H. P. Kelly, Phys. Rev. A **41**, 3612 (1990).
[14] J. A. Robertson, M. Kutzner, and P. Pelley, Phys. Rev. A **63**, 042715 (2001).
[15] M. Kutzner, J. A. Robertson, and P. Pelley, Phys. Rev. A **62**, 062717 (2000).
[16] W. R. Johnson and C. D. Lin, Phys. Rev. A **20**, 964 (1979); W. R. Johnson, C. D. Lin, K. T. Cheng, and C. M. Lee, Phys. Scr. **21**, 409 (1980).
[17] V. Radojević, M. Kutzner, and H. P. Kelly, Phys. Rev. A **40**, 727 (1989).
[18] M. Ya. Amusia, in *Atomic Photoeffect*, edited by P. G. Burke and H. Kleinpoppen (Plenum, New York, 1990).
[19] C. H. Greene and M. Aymar, Phys. Rev. A **44**, 1773 (1991); F. Robicheaux and C. H. Greene, *ibid.* **46**, 3821 (1992).
[20] R. J.-M. Pellenq and D. Nicholson, Mol. Phys. **95**, 549 (1998).
[21] I. P. Grant, B. J. McKenzie, P. H. Norrington, D. F. Mayers, and N. C. Pyper, Comput. Phys. Commun. **21**, 207 (1980).
[22] A. E. Hansen, Mol. Phys. **13**, 425 (1967).
[23] M. Kutzner and J. T. Brown (unpublished).
[24] J. Cooper and R. N. Zare, J. Chem. Phys. **48**, 942 (1968).